BUTTERWORTH HEINEMANN

Polymer Vol. 36 No. 12, pp. 2427–2433, 1995

0032-3861/95/$10.00 + 0.00

Surface segregation in blends of styrene–acrylonitrile copolymers

Eugene Kim*
Department of Chemistry, Baker Laboratory, Cornell University, Ithaca, NY 14853, USA

and Edward J. Kramer†
Department of Materials Science and Engineering, and the Materials Science Center, Cornell University, Ithaca, NY 14853, USA

and Paul D. Garrett, Robert A. Mendelson‡ and Wan C. Wu
The Chemical Group of Monsanto Company, 730 Worcester Street, Springfield, MA 01151, USA
(Received 26 May 1994; revised 24 October 1994)

We investigated the kinetic as well as thermodynamic aspects of surface segregation in blends of random copolymers of styrene and acrylonitrile (SAN) with different acrylonitrile contents (22.5 and 27.2 wt%) annealed at 163 C. A comparison was made with equilibrium data collected by Mansfield *et al.* on the same system using neutron reflectivity. The lower-AN-content SAN, which is labelled with deuterium (d-SAN), was observed to segregate to the vacuum/polymer interface. Time-of-flight and conventional forward recoil spectrometry were used to determine the depth profile of the deuterated component. The apparent diffusion coefficient D_{app} controlling the segregation kinetics at a bulk volume fraction ϕ of d-SAN of 0.34 was obtained. It was smaller by a factor of approximately 1.5 than the mutual diffusion coefficient $\tilde{D}$ at $\phi = 0.34$ calculated without taking the expected thermodynamic slowing of diffusion into account. However, D_{app} was larger than the measured $\tilde{D}$ at $\phi = 0.34$ by a factor of approximately 3. The mean-field theory of Schmidt and Binder was employed to extract the Flory interaction parameter χ, which was found to be smaller than but close to its critical value χ_c. The value of $\tilde{D}$ computed using this χ value was in good agreement with the independently measured $\tilde{D}$ at $\phi = 0.34$.

(Keywords: surface segregation; styrene–acrylonitrile; random copolymer)

INTRODUCTION

The surface composition in a multicomponent system is expected to be different from the bulk because each component generally has a different surface energy, γ. This segregation impacts practical properties such as adhesion, wetting and friction, so that understanding surface segregation has a technological as well as scientific importance. For polymers, this effect is amplified owing to a small combinatorial entropy of mixing, which means that even a small difference in the surface energy between the components can cause massive segregation. In the isotopic homopolymer blends, the thermodynamic[1-5] and kinetic[6] aspects of such a surface enrichment process have been studied in depth. However, only a limited number of investigations of surface enrichment in practical polymer blends can be found in the literature[7-9].

Random copolymers (SAN) of styrene (S) and acrylonitrile (AN) are some of the most widely used materials in the thermoplastics industry, for example as an ingredient in acrylonitrile–butadiene–styrene (ABS) resin. When SANs with different AN contents are mixed, the mixture forms one homogeneous phase until the AN content difference reaches about 5%[10]. For such miscible blends, however, the surface composition will not be the same as that of the bulk: the SAN with a lower AN content is expected to have weaker interchain bonding than the one with higher AN content owing to the polar nature of the AN unit. Thus the low-AN-content SAN molecule would be energetically favourable to place at the vacuum/polymer interface. Indeed, after annealing above the glass transition temperature, the surfaces of blends of SANs with different AN contents have been observed to be enriched in the lower-AN-content component[11]. We report the results on the kinetics and thermodynamics of surface enrichment in blends of SANs with 22.5 and 27.2 wt% AN contents using ion-beam depth-profiling techniques (time-of-flight and conventional forward recoil spectrometry). The formulations used for discussing the experimental findings will be briefly presented in the rest of this section.

Kinetics

The kinetics of the surface segregation process has been studied by assuming that the growth of the layer is

*Present address: Department of Science, Hong Ik University, Mapo-ku, Sangsoo-dong 72-1, Seoul, Korea
†To whom correspondence should be addressed
‡Present address: Exxon Chemical Company, Baytown Polymer Center, 5200 Baywat Drive, Baytown, TX 77522-5200, USA

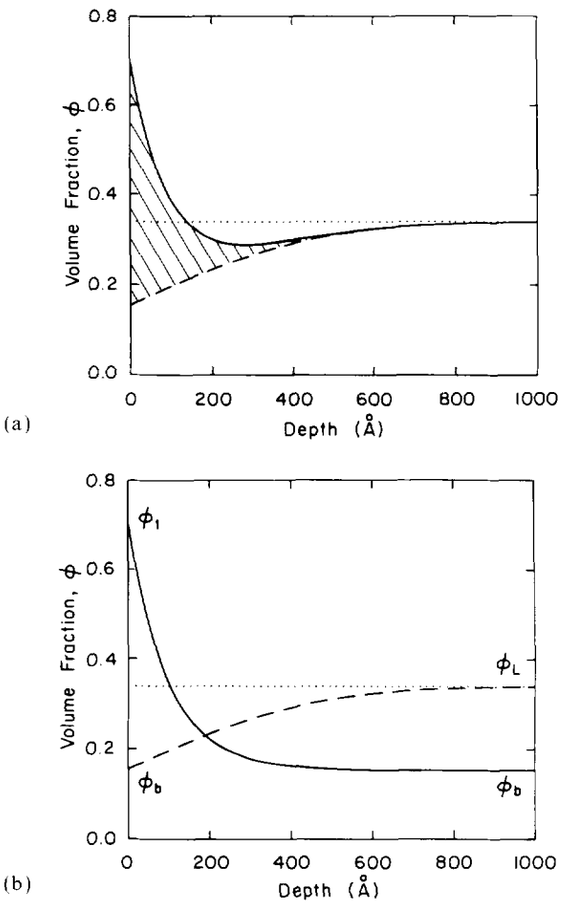

Figure 1 (a) The surface enrichment profile obtained according to equation (4) (full curve). The broken curve and dotted line represent the depletion profile $\phi_d(x)$ and the profile before annealing. The diffusion distance $w=(4D_{app}t)^{1/2}$ was 500 Å and the parameters used for determining $\phi_s(x)$ are explained in the text. The hatched area indicates $z^*=53$ Å. (b) The full curve represents the exponentially decaying surface segregation profile $\phi_s(x)$. The broken curve and dotted line are the same as those in (a). The surface volume fraction (ϕ_1), the volume fraction at $x=L$ (ϕ_L) and the volume fraction at the hypothetical local boundary (ϕ_b) are also shown

diffusion-limited[6,12]. In this section, the original idea proposed by Jones and Kramer[6] is applied to derive a simple analytical expression for the shape of the non-equilibrium surface profile, utilizing information obtained from equilibrium depth profiles (the integral surface excess z^* and the surface volume fraction ϕ_1). Initially, when the lower-surface-energy component segregates to the surface, a zone behind the surface layer is depleted in that component. The resulting concentration gradient drives diffusion from the bulk to this depleted zone, while the surface layer is built up at the same time (*Figure 1a*). Under such circumstances the segregated amount of the material at the surface would be controlled by the diffusion distance, $w(4D_{app}t)^{1/2}$, where D_{app} is the 'apparent' diffusion coefficient, which accounts for the segregation process, and t is the annealing time. The following two regions are assumed to be in local equilibrium: the segregating region and the depleted region from which the segregating component is being supplied. We consider the situation where the diffusion distance is so much greater than the characteristic size of the enriched layer that the boundary that divides the two regions can be approximately fixed at the surface during the process†. When the total film thickness L is of the same order of magnitude as w, the profile for the depletion $\phi_d(x)$ can be obtained using an error-function series[13]:

$$\phi_d(x)=\phi_L-(\phi_L-\phi_b)\left[\sum_{n=0}^{\infty}(-1)^n\,\mathrm{erfc}\left(\frac{2nL+x}{w}\right)+\sum_{n=0}^{\infty}(-1)^n\,\mathrm{erfc}\left(\frac{(2n+2)L-x}{w}\right)\right] \quad (1)$$

where x is the distance from the surface, ϕ_L is the volume fraction at $x=L$ (we distinguish it from ϕ_∞, which will denote the equilibrium bulk composition) and ϕ_b is the volume fraction at the boundary (fixed at $x=0$). Using conservation of mass (the surface excess z^* is equal to the amount of depletion from the bulk concentration), the following relation is obtained:

$$z^*=\int_0^\infty[\phi_L-\phi_d(x)]\mathrm{d}x\approx(\phi_L-\phi_b)\int_0^\infty\mathrm{erfc}(x/w)\mathrm{d}x \quad (2)$$

Equation (2) is rearranged to yield

$$\phi_L-\phi_b-\pi^{1/2}z^*/w\approx 0 \quad (3)$$

where $z^*=z^*(\phi_b)$ is obtained from the surface excess at equilibrium when the concentration in the bulk is ϕ_b. The above equation is solved for ϕ_b (*Figure 1b*). The overall profile $\phi(x)$ is obtained by summing $\phi_d(x)$ (equation (1), broken curve in *Figure 1b*) and the surface-segregating profile $\phi_s(x)$ (full curve in *Figure 1b*) less ϕ_b:

$$\phi(x)=\phi_d(x)+\phi_s(x)-\phi_b \quad (4)$$

The details of how we obtained $\phi_s(x)$ will be explained in the section on 'Kinetics' in the 'Discussion'. *Figure 1a* shows the example of such a profile, and the hatched area indicates z^*. After taking the limited depth resolution of our experiments into account, D_{app} can be obtained by a comparison of the theoretical and experimental profiles.

Thermodynamics

The equilibrium composition profile near the surface can be established by balancing the free energy gained by putting the lower-surface-energy component at the surface with the free energy penalties for creating a gradient in concentration and for maintaining a local composition different from the bulk. This problem has been solved using a mean-field approximation[14,15]. We briefly summarize the consequences of the theory using the Schmidt and Binder notation[14]. The theory has been successful in interpreting many surface segregation phenomena[1,5,8,9,16] observed recently including results on surface excess z^* and surface volume fraction ϕ_1.

†The very initial process during which this boundary rapidly shifts to this distance of $w=(4D_{app}t)^{1/2}$ was not accounted for in the present formulation. However, fixing the boundary in this way turned out to be a reasonable assumption shortly after the depleted layer is formed, because most of the diffusion takes place with only a small displacement of this boundary (less than a radius of gyration, which is ~110 Å for d-SAN-EF); for example w is 1530 Å in *Figure 3*

Table 1 Acrylonitrile (AN) content, weight-average molecular weight and polydispersity indices of deuterated and protonated poly(styrene-*co*-acrylonitrile)

	AN (wt%)	M_w (g mol^{-1})	M_w/M_n
d-SAN-EF	22.6	1.8×10^5	2.2
d-SAN-GH	22.4	1.1×10^5	2.0
SAN-23	22.9	1.8×10^5	3.0
SAN-27	27.2	2.4×10^5	2.4

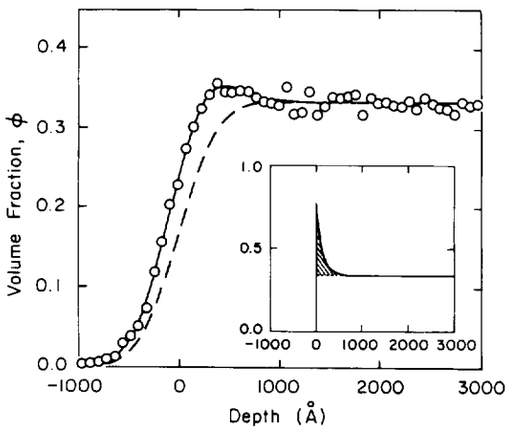

Figure 2 The concentration profile of d-SAN-GH in the blend of d-SAN-GH and SAN-27 measured by conventional f.r.e.s. The sample was annealed at 163 C for 2 weeks ($z^*=54$ Å). The inset shows the predicted exponentially decaying profile, which was convolved with a Gaussian with a f.w.h.m. of 730 Å (full curve drawn through the data points). The broken curve represents the unannealed profile (convolved step profile). The values of surface concentration ϕ_1 and correlation length ξ_χ were 0.76 and 129 Å, respectively, obtained from the broken curves in *Figures 4* and *5*

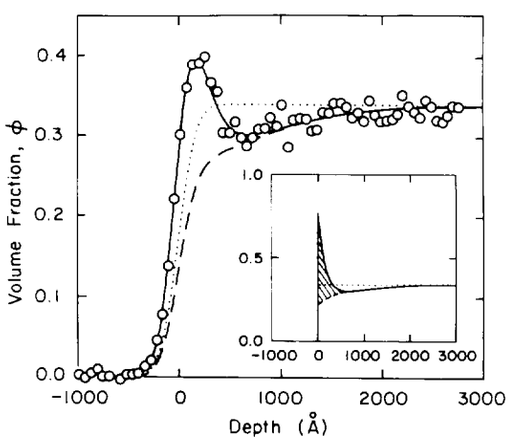

Figure 3 The concentration profile of d-SAN-EF in the blend of d-SAN-EF and SAN-27 measured by t.o.f.-f.r.e.s. The sample was annealed at 163 C for 9 h ($w=1530$ Å and $z^*=88$ Å). The inset shows the predicted profile according to equation (4), which was convolved with a Gaussian with a f.w.h.m. of 300 Å (full curve drawn through the data points). The broken curve represents $\phi_d(x)$ given in equation (3). The apparent diffusion coefficient D_{app} of 1.7×10^{-15} cm^2 s^{-1} could be extracted by fitting the surface excess and slope of the data points. The dotted curve represents the unannealed profile (convolved step profile). The parameters used for determining the exponentially decaying surface segregation profile $\phi_s(x)$ are explained in the text

From the theory the surface excess z^* is found to be [1,16]:

$$z^*=\frac{a}{6}\int_{\phi_1}^{\phi_s}\frac{\phi-\phi_x}{\{\phi(1-\phi)[\Delta G(\phi)-\Delta G(\phi_x)-(\phi-\phi_x)\Delta\mu(\phi_x)]\}^{1/2}}\mathrm{d}\phi \quad (5)$$

where ϕ_x is the volume fraction of lower-surface-energy component in the bulk, ΔG is the Flory–Huggins free energy of mixing ($\Delta\mu$ is the derivative of ΔG with respect to ϕ) and a is the statistical segment length, which was taken to be 6.1 Å from the neutron scattering experiments[17] on SAN with 19 wt% AN. When z^* and ϕ_1 are known as a function of ϕ_x, the Flory interaction parameter χ in ΔG is the only unknown parameter and can be extracted.

The surface energy difference $\Delta\gamma$ can also be derived[14] by an approximation that it would be a linear function of ϕ_1 (refs. 1, 5):

$$\Delta\gamma=-\frac{akT}{3b^3}\left[\frac{\Delta G(\phi_1)-\Delta G(\phi_x)-(\phi_1-\phi_x)\Delta\mu(\phi_x)}{\phi_1(1-\phi_1)}\right]^{1/2} \quad (6)$$

where b is a unit-cell dimension of the Flory–Huggins lattice, which is calculated to be 5.1 Å from the molecular weight of the monomer and its density. In the section on 'Surface energy difference' in the 'Discussion' we will evaluate $\Delta\gamma$ using equation (6) and the validity of the approximation on $\Delta\gamma$ will be discussed.

EXPERIMENTAL

Protonated SAN with 27.2 wt% AN content with weight-average molecular weight M_w of 240 000 (SAN-27) was blended with one of two deuterated SAN (d-SAN) having nearly the same AN content (~22.5 wt%) but different M_w values (M_w(d-SAN-EF) = 180 000, M_w(d-SAN-GH) = 110 000). They are tabulated in *Table 1* with their polydispersity indices. The d-SAN were prepared by polymerizing acrylonitrile and perdeuterated styrene monomers using t-butyl peroctoate as free-radical initiator and terpinolene as a chain-transfer agent. The details of synthesis are discussed elsewhere[18].

The polymers were dissolved in methyl isobutyl ketone and the films of binary blends (d-SAN-EF/SAN-27 and d-SAN-GH/SAN-27) with thicknesses of more than 1 μm were spun-cast onto the silicon wafer. These were first dried and then annealed at 163°C for various times up to 2 weeks. The depth profile was obtained using either conventional or time-of-flight (t.o.f.) forward recoil spectrometry (f.r.e.s.). The predicted profile (equation (4)) was convolved with a Gaussian function with a full width at half-maximum (f.w.h.m.) of 740 Å for conventional f.r.e.s. and 300 Å for t.o.f.-f.r.e.s. to take into account the depth resolution. The enhanced resolution in t.o.f.-f.r.e.s. comes from the ability to remove a stopper foil, which was required in conventional f.r.e.s. to keep the elastically scattered $^4He^{2+}$ particles from reaching the detector[19,20].

Figure 2 shows an example of the equilibrium surface segregation profile in the blend of d-SAN-GH and SAN-27 annealed at 163°C for 2 weeks. The predicted structure of the actual profile (inset) can hardly be seen owing to the poor resolution, but the surface excess z^*

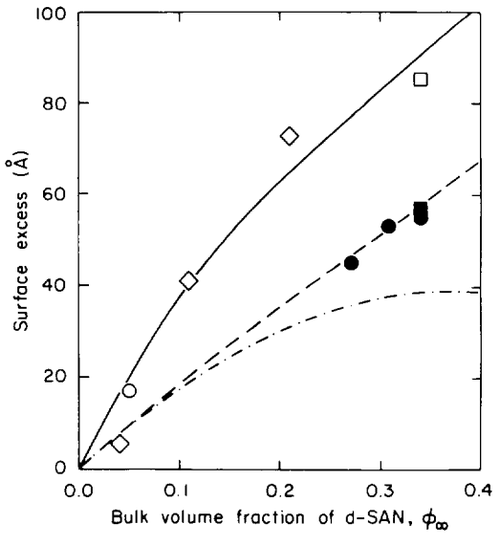

Figure 4 The equilibrium surface excess z^* as a function of bulk volume fraction ϕ_∞ for two different molecular weights of d-SAN mixed with SAN-27 using various techniques. For d-SAN-EF, neutron reflectometry[11] (◇), time-of-flight forward recoil spectrometry t.o.f.-f.r.e.s. (□) and conventional f.r.e.s. (○) were used; and for d-SAN-GH, t.o.f.-f.r.e.s. (■) and conventional f.r.e.s. (●) were used. The full and broken curves represent the prediction according to equation (5): $\chi = 8.2 \times 10^{-4}$ and $\chi = 10.6 \times 10^{-4}$ were used for d-SAN-EF/SAN-27 and d-SAN-GH/SAN-27 blend, respectively. The chain curve represents the prediction for d-SAN-GH when $\chi = 8.2 \times 10^{-4}$. To obtain the surface volume fraction ϕ_1 needed for these predictions, the data in *Figure 5* were used. Refer to the text for details

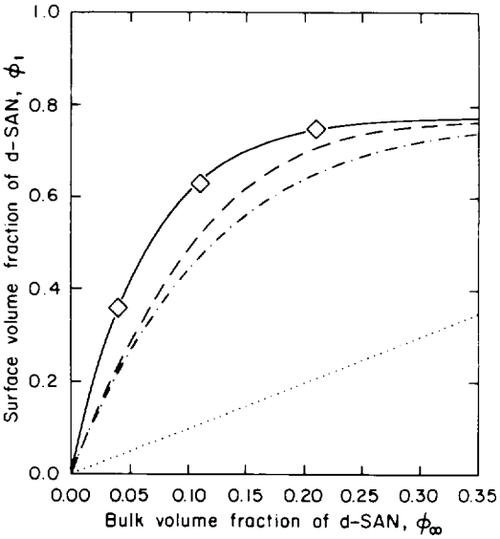

Figure 5 Surface volume fraction ϕ_1 measured using neutron reflection by Mansfield *et al.*[11] is plotted as a function of the bulk volume fraction ϕ_∞. The full curve is the non-linear least-squares fit to the data using the functional form of $a[1\text{-exp}(-x/b)]$ (where $a = 0.779$ and $b = 0.0654$). The broken and chain curves are the calculated values of ϕ_1 for d-SAN-GH using $\chi = 10.6 \times 10^{-4}$ and 8.2×10^{-4}, respectively, assuming the same surface energy difference given in *Figure 8*. Refer to the text for the details. The dotted line represents the line $\phi_1 = \phi_\infty$

could be measured accurately with this technique. In contrast as seen in *Figure 3* (the blend of d-SAN-EF and SAN-27; annealed at 163°C for 9 h), with the better instrumental resolution of t.o.f.-f.r.e.s., one could see more details of the change in concentration near the surface, including a depletion layer below the surface-enriched layer. The full curve through the data is based on the profile shown in the inset, using the form of equation (4). From this profile, D_{app} could be extracted.

The mutual diffusion coefficient $\tilde{D}$ in the blend of d-SAN and SAN-27 at $\phi = 0.34$ was measured by monitoring the broadening of the interface between the two layers, which were prepared by putting the top layer of about 3000 Å thickness with $\phi = 0.32$ on a bottom layer with $\phi = 0.36$. To minimize the influence of the composition dependence on diffusion, $\Delta\phi$ was made small. Details of this procedure may be found elsewhere[21].

RESULTS

We first examined the blend of d-SAN and SAN of $M_w = 180\,000$ with a similar AN content (22.9 wt%). No surface excess was detected†. The equilibrium values of z^* in the blends of d-SAN and SAN-27 at 163°C are shown in *Figure 4*. Data obtained using t.o.f. and conventional f.r.e.s. together with the neutron reflectometry (n.r.) data by Mansfield *et al.*‡ are plotted as open symbols for d-SAN-EF and as filled symbols for d-SAN-GH. The neutron reflectiviy (n.r.) is extremely sensitive to sharp changes in the scattering length density profile, enabling the value of ϕ_1 to be extracted accurately from the reflectivity data at large wavevectors[11]. Mansfield's n.r. data on the surface volume fraction ϕ_1 *versus* ϕ_∞ are shown in *Figure 5*.

The mutual diffusion coefficients $\tilde{D}$ in the blend of d-SAN and SAN-27 at $\phi = 0.34$ are shown as open and filled circles with error bars in *Figure 6* for d-SAN-EF and d-SAN-GH, respectively. The tracer diffusion coefficients D^* of d-SAN in SAN-27 have also been measured[18]. These are shown as open and filled circles at $\phi = 0$ in *Figure 6* for d-SAN-EF and d-SAN-GH, respectively.

DISCUSSION

Kinetics

We first considered the blend of d-SAN-EF and SAN-27, the same materials that Mansfield *et al.* used in their neutron reflectometry (n.r.) investigation[11]. The equilibrium profile $\phi_{equil}(x)$, which is also $\phi_s(x)$ in equation (4) when $\phi_b = \phi_\infty$, was taken as an exponentially decaying function from ϕ_1 to ϕ_∞, which approximates well the result of the mean-field theory of Schmidt and Binder[5,14,19]:

$$\phi_{equil}(x) = (\phi_1 - \phi_\infty)\exp(-x/\xi_s) + \phi_\infty \qquad (7)$$

The correlation length ξ_s as a function of ϕ_∞ could be calculated from the experimental z^* (full curve in *Figure 4*) and ϕ_1 (full curve in *Figure 5*) as follows, and is shown as a full curve in *Figure 7*:

$$\xi_s = z^*/(\phi_1 - \phi_\infty) \qquad (8)$$

†Our observation shows that partial deuterium substitution in those molecular-weight SAN polymers does not afford enough thermodynamic gain at the surface to overcome the entropic cost for creating a gradient at the surface

‡The temperature at which Mansfield annealed his samples was 167°C (ref. 11) rather than 163 C. We ignored this difference

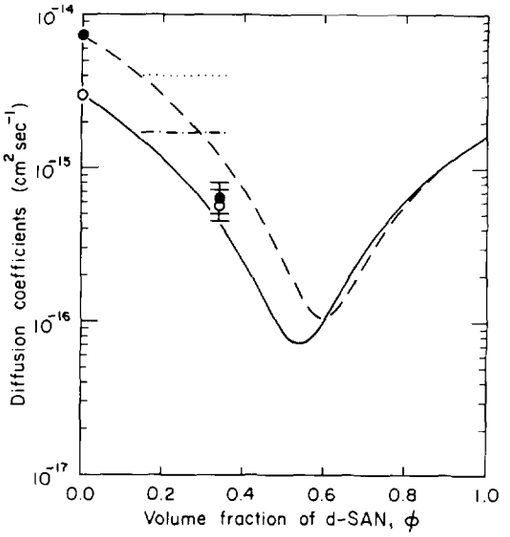

Figure 6 Various diffusion coefficients as a function of volume fraction ϕ of d-SAN: the apparent diffusion coefficients D_{app} for d-SAN-EF/SAN-27 blend (1.7×10^{-15} cm^2 s^{-1}, chain line) and for d-SAN-GH/SAN-27 blend (4.0×10^{-15} cm^2 s^{-1}, dotted line); predicted mutual diffusion coefficients $\tilde{D}$ from equation (12) for d-SAN-EF/SAN-27 blend (full curve) and for d-SAN-GH/SAN-27 blend (broken curve); measured tracer diffusion coefficients D^* in SAN-27 of d-SAN-EF (open circle at $\phi = 0$) and of d-SAN-GH (filled circle at $\phi = 0$); and measured $\tilde{D}$ at $\phi = 0.34$ for d-SAN-EF/SAN-27 blend (open circle with error bar) and for d-SAN-GH/SAN-27 blend (filled circle with error bar)

We note that this ξ_s has the experimental value of ϕ_1 embedded in it, in contrast with the one which would be predicted from the value of z^* only in the absence of ϕ_1 data using the Schmidt and Binder theory[1,3]. There will be more discussion on ξ_s and ϕ_1 in the following subsections on 'Correlation length' and 'Surface energy difference'.

The full curve in *Figure 3* is the profile obtained by matching z^* and the $\phi(x)$ given by equation (4) to the t.o.f.-f.r.e.s. depth profile of the d-SAN-EF/SAN-27 blend annealed at 163°C for 9 h ($w = 1530$ Å and $z^* = 88$ Å). The diffusion coefficient D_{app} of 1.7×10^{-15} cm^2 s^{-1} was extracted. The same procedure using samples annealed for 4.5 and 54 h gave a similar number for D_{app} within experimental error. This value will be compared with the diffusion coefficients obtained independently in the next section.

Interaction parameter and diffusion coefficients

The Flory interaction parameter χ in the blend of d-SAN-EF and SAN-27 was extracted using equation (5) to fit the z^* *versus* ϕ_x data. In *Figure 4* the full curve was drawn through the open symbols using $\chi = 8.2 \times 10^{-4}$ and $\phi_1(\phi_x)$ shown in *Figure 5*. Cowie and Lath proposed the following relation for χ in random copolymer blends[22,23]:

$$\chi = (x - y)^2 \chi_{S\text{-}AN} \tag{9}$$

where $\chi_{S\text{-}AN}$ is the 'common' binary interaction parameter between S and AN units, and x and y are the mole fractions of one of the component monomers of each SAN. They estimated $\chi_{S\text{-}AN}$ to be 0.76 from Molau's phase separation observations[10]. According to equation (9), χ is calculated to be 13.4×10^{-4} from our AN content difference, which is in reasonable agreement with the value extracted from z^* data. The χ we obtained (8.2×10^{-4}) was close to but smaller than χ at the critical point χ_c ($= 8.5 \times 10^{-4}$), which is given as:

$$\chi_c = \frac{(N_A^{1/2} + N_B^{1/2})^2}{2N_A N_B} \tag{10}$$

At our experimental temperature (163°C), the system is therefore in the one-phase region over all compositions because χ is always smaller than its value at spinodal (χ_s):

$$\chi_s = \frac{1}{2}\left(\frac{1}{\phi_A N_A} + \frac{1}{\phi_B N_B}\right) \tag{11}$$

On the other hand, this also suggests that it is impossible for a wetting (or pre-wetting) layer to grow within a framework of mean-field theory, and, in fact, no difference in z^* was observed by increasing the annealing time after z^* reached its expected equilibrium level. However, since our blend system approaches the critical point as ϕ_x becomes closer to the critical composition ϕ_c (and therefore as ϕ_1 increases), it is expected that deviations from the mean-field behaviour will become important. We note that the blend at ϕ_c would provide a model system for studying other thermodynamic or mechanical behaviour close to the critical point in the one-phase region.

The mutual diffusion coefficient $\tilde{D}$ was then calculated from the following equation[24,25]:

$$\tilde{D} = 2(\chi_s - \chi)\phi_A \phi_B (\phi_B D_A^* N_A + \phi_A D_B^* N_B) \tag{12}$$

where N_i is the degree of polymerization and ϕ_i is the volume fraction of component i. Assuming that the monomer friction coefficient ζ_0 of SAN-27 in d-SAN is

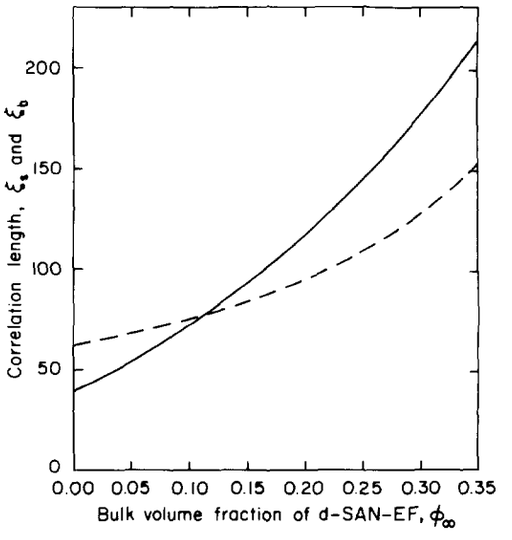

Figure 7 The surface correlation length ξ_s obtained from equation (8) (full curve) and the bulk correlation length ξ_b obtained from equation (11) (broken curve) in the blend of d-SAN-EF and SAN-27 as a function of bulk volume fraction ϕ_x of d-SAN-EF

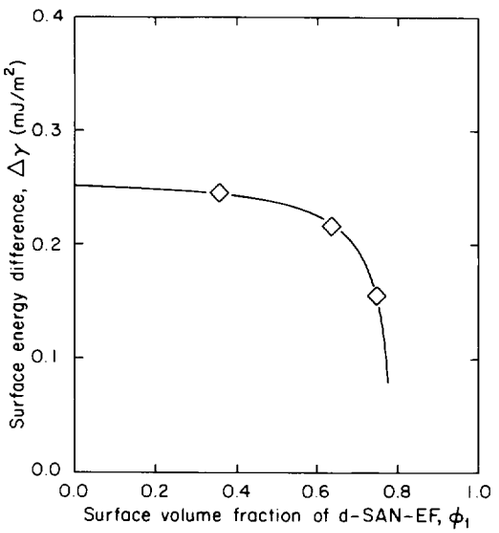

Figure 8 The surface energy difference $\Delta\gamma$ (mJ m^{-2}) ($\diamond$) as a function of surface volume fraction ϕ_1 of d-SAN-EF in the blend of d-SAN-EF and SAN-27. These were calculated according to equation (6) using $\chi = 8.2 \times 10^{-4}$ and using the ϕ_1 *versus* ϕ_s relation appearing in *Figure 5*. The full curve represents the values calculated from the full curve in *Figure 5*

the same as that of d-SAN in SAN-27† and using reptation scaling‡ ($D^* \sim M^{-2}$), we estimated D^* of SAN-27 into d-SAN-EF. The resulting $\tilde{D}$ as a function of d-SAN-EF volume fraction ϕ is plotted in *Figure 6* (full curve). The $\tilde{D}$ at $\phi = 0.34$ measured independently (open circle with error bar) agrees well with the $\tilde{D}$ prediction. The chain line represents the D_{app} obtained from the surface segregation kinetics ($= 1.7 \times 10^{-15}$ cm^2 s^{-1}). From equation (12) we estimated the $\tilde{D}$ at $\phi = 0.34$ when $\chi = 0$, which was 2.5×10^{-15} cm^2 s^{-1} (D^* of d-SAN-EF was 3.0×10^{-15} cm^2 s^{-1}). The value of D_{app} is smaller than this by a factor of about 1.5. This decrease might be attributed to thermodynamic slowing of diffusion as a result of the positive value of χ. However, D_{app} was significantly larger than $\tilde{D}$ at $\phi = 0.34$ either measured or calculated using this χ by a factor of about 3.

We take note of several points on the interpretation of D_{app}. First, the polymers that we used had polydispersity indices larger than 2 (*Table 1*). Shorter chains, as a result, would migrate faster towards the surface than longer ones. At the same time, such a process would be favoured owing to smaller free-energy penalty at the surface for reducing conformational freedom[27,28] as well as for creating a density gradient[29], which becomes important in the small-χ system. Secondly, in the region of local equilibrium when d-SAN is being supplied from the bulk to the surface (*Figure 1*), ϕ is smaller than 0.34 especially in the initial stages of the process. Mutual diffusion depends strongly on composition as seen in *Figure 6* and this might partly account for the fact that D_{app} is larger than $\tilde{D}$.

Correlation length

We computed the bulk correlation length ξ_b from the following equation[30,31]:

$$\xi_b = \frac{1}{6} a[\phi(1-\phi)(\chi_s - \chi)]^{-0.5} \qquad (13)$$

Equation (13) is represented by the broken curve in *Figure 7* and it is compared wih the surface correlation length ξ_s (full curve). They approximately agree in magnitude, but the surface correlation length is shown to vary more strongly with composition. We note that the ξ_s would be accurate only if the surface enrichment profile is the exponentially decaying function given in equation (7). Polydispersity, distortion of the chain conformation at the surface, and imperfectly random dispersion of AN groups (blockiness) might induce some deviation from the predicted profile. However, our resolution would not allow us to see those slight differences. Mansfield's n.r. results also showed that equation (7) is not a perfect description.

Surface energy difference

We also calculated the surface energy difference $\Delta\gamma$ (equation (6)) as a function of ϕ_1 for the given χ and ϕ_s, and these values are plotted in *Figure 8*. The difference in surface energy was found to be about 0.25 mJ m^{-2} at ϕ_1 of about 0.4. This is significantly smaller (by more than an order of magnitude) than the values in practical polymer blends[16], and is a little larger than the values found in isotopic polymer blends (for example, the surface energy differences between d-polystyrene and polystyrene[1,3] and between d-poly(ethylene–propylene) and poly(ethylene–propylene)[4] are about 0.08 and 0.2 mJ m^{-2}, respectively). Interestingly, it tends to decrease with increasing ϕ_1, which means that the preference for lower-AN-content SAN at the surface diminishes. This trend contrasts to the finding by Zhao *et al.*[3] in the blend of d-polystyrene and polystyrene that $\Delta\gamma$ increased sharply for $\phi_1 > 0.6$. These results show that the approximation that $\Delta\gamma$ is a linear function of ϕ_1 is questionable. Zhao *et al.* discussed the possible origin of the discrepancy considering extra surface entropy factors. However, it is not obvious why our $\Delta\gamma$ extracted in this copolymer blend system decreases with increasing ϕ_1.

Molecular-weight dependence of surface segregation

We also investigated the surface segregation in the blend of d-SAN-GH and SAN-27 (*Table 1*). Because the data on ϕ_1 were not available in this case, the z^* data (filled symbols in *Figure 4*) were fitted to equation (7) as a function of ϕ_s using the ϕ_1 *versus* ϕ_s relation obtained from the assumption that the surface energy difference at a given ϕ_1 is the same as that in the d-SAN-EF/SAN-27 blend (*Figure 8*). A χ of 10.6×10^{-4} fits the data best (broken curve in *Figure 4*), while $\chi = 8.2 \times 10^{-4}$, which was the value in the d-SAN-EF/SAN-27 blend, gives rise to smaller z^* values (chain curve). We also note that the χ in d-SAN-GH/SAN-27 blends is quite close to the value of χ_c ($= 10.9 \times 10^{-4}$) and in good agreement with the value obtained using equation (9) ($= 14.7 \times 10^{-4}$). The

†This assumption was partly supported by the facts that ζ_0 of d-SAN in SAN-27 was identical to that of d-SAN in SAN with the same AN content (ref. 18)

‡The molecular weight of d-SAN-EF was smaller than SAN-27 (*Table 1*) and D^*_{SAN27} may have a dependence on molecular weight of the matrix. We calculated the contribution of the constraint release[26] using the number of suitably situated constraints to be 3.5. Only a 3% increase in D^* compared with the self-diffusion coefficient of SAN-27 was obtained. This influence will be even smaller as SAN-27 concentration increases

calculated values of ϕ_1 for d-SAN-GH as a function of ϕ_x are also shown in *Figure 5* as a broken curve (using $\chi = 10.6 \times 10^{-4}$) and as a chain curve (using $\chi = 8.2 \times 10^{-4}$)†.

We also could extract the D_{app} ($= 4.0 \times 10^{-15}$ cm^2 s^{-1}) utilizing the intermediate segregation profiles and the above information on equilibrium. The D_{app} (dotted line) and predicted $\tilde{D}$ from equation (12) (broken curve) are shown in *Figure 6*, together with the $\tilde{D}$ measured independently (filled circle with error bar at $\phi = 0.34$) and the D^* of d-SAN-GH into SAN-27 (filled circle at $\phi = 0$). They show the same trend as we saw in the d-SAN-EF and SAN-27 blend: D_{app} is a little smaller than the predicted $\tilde{D}$ when $\chi = 0$, but significantly larger than the measured or predicted $\tilde{D}$.

CONCLUSIONS

Low-AN-content SAN segregates to the surface. Surface segregation of low-M_w SAN is smaller than that of high-M_w SAN. When the kinetics of surface segregation is assumed to be diffusion-limited, D_{app} could be extracted, which was observed to be larger than $\tilde{D}$ at the bulk concentration. The surface energy difference between d-SAN with 22.6 wt% AN content and SAN with 27.2 wt% SAN is ~ 0.25 mJ m^{-2} at a surface volume fraction ϕ_1 of d-SAN of $\phi_1 \simeq 0.4$ and decreases with ϕ_1.

ACKNOWLEDGEMENTS

This work was supported by the Division of Materials Research, NSF Polymers Program Grant No. DMR-9223099 and by fellowship support from Monsanto Chemical Co. through the Polymer Outreach Program of the Materials Science Center at Cornell University. The authors thank T. Mansfield for providing the neutron reflectivity data. We are grateful to L. Norton for providing unpublished data on the surface segregation experiment in the isotopic blend of poly(ethylene–propylene) and for discussion.

†Jones and Kramer indicated in ref. 16 that for most chemically dissimilar polymer blends, which usually have a surface energy difference $\Delta\gamma$ of much greater than 2 mJ m^{-2}, z^* and ϕ_1 are insensitive to χ, while it is illustrated here that z^* and ϕ_1 are rather sensitive to χ, because of the small magnitude of $\Delta\gamma$ (< 0.25 mJ m^{-2})

REFERENCES

1 Jones, R. A. L., Kramer, E. J., Rafailovich, M. H., Sokolov, J. C. and Schwarz, S. *Phys. Rev. Lett.* 1989, **62**, 280
2 Jones, R. A., Norton, L. J., Kramer, E. J., Composto, R. J., Stein, R. S., Russell, T. P., Mansour, A., Karim, A., Felcher, G. P., Rafailovich, M. H., Sokolov, J., Zhao, X. and Schwarz, S. A. *Europhys. Lett.* 1990, **12**, 41
3 Zhao, X., Zhao, W., Sokolov, J., Rafailovich, M. H., Schwartz, S. A., Wilkens, B. J., Jones, R. A. L. and Kramer, E. J. *Macromolecules* 1991, **24**, 5991
4 Norton, L. J., Kramer, E. J., Bates, F. S., Gehlsen, M. D., Jones, R. A. L., Karim, A., Felcher, G. P. and Kleb, R. submitted
5 Jones, R. A. L., Kramer, E. J., Rafailovich, M. H., Sokolov, J. and Schwarz, S. A. *Mater. Res. Soc. Symp. Proc.* 1989, **153**, 133
6 Jones, R. A. and Kramer, E. J. *Phil. Mag. (B)* 1990, **62**, 129
7 Bhatia, Q. S., Pan, D. A. and Koberstein, J. T. *Macromolecules* 1988, **21**, 2166
8 Sakellariou, P. *Polymer* 1993, **34**, 3408
9 Cowie, J. M. G., Devlin, B. G. and McEwen, I. J. *Macromolecules* 1993, **26**, 5628
10 Molau, G. E. *Polym. Lett.* 1965, **3**, 1007
11 Mansfield, T., Ph.D. Thesis, University of Massachusetts, Amherst, MA, 1993; Mansfield T., Stein, R. S., Composto, R. J., Rafailovich, M. H. and Sokolov, J. *Physica (B)* 1991, **173**, 207; Composto, R. J., Mansfield, T. L., Stein, R. S., Felcher, G. P. and Karim, A. *Polym. Prepr., Am. Chem. Soc., Div. Polym. Chem.* 1990, **31**(2), 137
12 Lipowsky, R. and Huse, D. A. *Phys. Rev. Lett.* 1986, **57**, 353
13 Crank, J. 'The Mathematics of Diffusion', 2nd Edn., Clarendon Press, Oxford, 1975
14 Schmidt, I. and Binder, K. *J. Physique* 1985, **46**, 1631
15 Nakanishi, H. and Pincus, P. *J. Chem. Phys.* 1983, **79**, 997
16 Jones, R. A. L. and Kramer, E. J. *Polymer* 1993, **34**, 115
17 Schmitt, B. J., Kirste, R. G. and Jelenic, J. *Makromol. Chem.* 1980, **181**, 1655
18 Kim, E., Kramer, E. J., Garrett, P. D., Mendelson, R. A. and Wu, W. C. *J. Mater. Sci.* in press
19 Sokolov, J., Rafailovich, M. H., Jones, R. A. L. and Kramer, E. J. *Appl. Phys. Lett.* 1989, **54**, 590
20 Kramer, E. J. *Physica (B)* 1991, **173**, 189
21 Composto, R. J., Kramer, E. J. and White, D. M. *Macromolecules* 1988, **21**, 2580
22 ten Brinke, G., Karasz, F. E. and MacKnight, W. J. *Macromolecules* 1983, **16**, 1827
23 Cowie, J. M. C. and Lath, D. *Makromol. Chem., Macromol. Symp.* 1988, **16**, 103
24 Kramer, E. J., Green, P. F. and Palmstrom, C. J. *Polymer* 1984, **25**, 473
25 Sillescu, H. *Makromol. Chem., Rapid Commun.* 1987, **8**, 393
26 Graessley, W. W. *Adv. Polym. Sci.* 1982, **47**, 67
27 Hariharan, A., Kumar, S. K. and Russell, T. P. *Macromolecules* 1990, **23**, 3584
28 Kumar, S. K. and Russell, T. R. *Macromolecules* 1991, **24**, 3816
29 Hariharan, A., Kumar, S. K. and Russell, T. P. *J. Chem. Phys.* 1993, **98**, 4163
30 Binder, K. *J. Chem. Phys.* 1983, **79**, 6387
31 Shibayama, M., Tang, H., Stein, R. S. and Han, C. C. *Macromolecules* 1985, **18**, 2179